

Crystallization During Fast Cooling Experiments, a Novel Apparatus for Real Time Monitoring

Valerio Brucato, Felice De Santis, Angelo Giannattasio, Gaetano Lamberti and Giuseppe Titomanlio*

Department of Chemical and Food Engineering, University of Salerno
Via Ponte don Melillo, I-84084 Fisciano (SA), Italy
*Phone +39089964026, Fax +39089964057, e-mail: glamberti@unisa.it

Summary: Although many efforts have been spent on polymer crystallization kinetics, reliable results, if typical industrial processing conditions are applied, have been attained only in few cases.

The main problem is related to the availability of data obtained under fast cooling conditions. Only those data can indeed discriminate between available models, or lead to the development of new ones.

A new apparatus, able to provide real time crystallization data under high cooling rates, has been designed, built and tested. Description of apparatus and methods are discussed together with preliminary data obtained.

Introduction

Description of polymer transformation processes requires a good knowledge of material crystallization kinetics, under conditions that are very different with respect to usual conditions which available data normally found in literature refer to. During industrial processing, indeed, polymeric materials are subjected to high cooling rates; moreover often high pressures, high shear and/or elongational rates are also applied.

Knowledge of crystallinity evolution in quiescent conditions and under high cooling rates is the starting point for the modeling of effects of flow on crystallization kinetics. In particular it is well known that crystallization kinetics increases by effect of flow and a comparison of crystallinity evolution under quiescent and flow conditions, at the same cooling rate, is the only way to discriminate between cooling and flow effects. From this point of view the investigation of quiescent crystallization kinetics under cooling rates of the order of those experienced during processing operations is very relevant to the study of flow induced crystallization evaluation and its modeling.

Recently an attempt to obtain real time crystallization data during fast cooling has been performed by developing the depolarized light detection technique^[1, 2], early proposed by Magill in the sixties. The real time crystallinity detection technique was successfully applied to an iPP resin adopting cooling rates larger than the maximum cooling rate

attainable in a standard DSC by a factor of about 3, cooling rates normally experienced by a resin during polymer processing are still much larger than those attained during those experiments.

High cooling rates, comparable with those experienced by the polymer during industrial processes, have been obtained by researchers of University of Palermo^[3-5] in an home made device. Information collected by that investigation was, however, limited to the analysis of polymer samples solidified under known high cooling rates. A much more powerful piece of information would be the knowledge of crystallinity evolution during sample cooling, attained by real time monitoring.

The purpose of this work is to set up and validate an apparatus and a method able to provide reliable real time experimental data of polymer crystallization under the effect of high cooling rates, and eventually to compare crystallinity evolution under quiescent conditions with crystallinity evolution, at the same cooling rate, under the effect of flow.

Experimental

Material

The resin adopted for the experiments performed in this work is a commercial iPP supplied by Montell (T30G, $M_w = 481000$, $M_n = 75000$, tacticity = 87.6%*mmmm*).

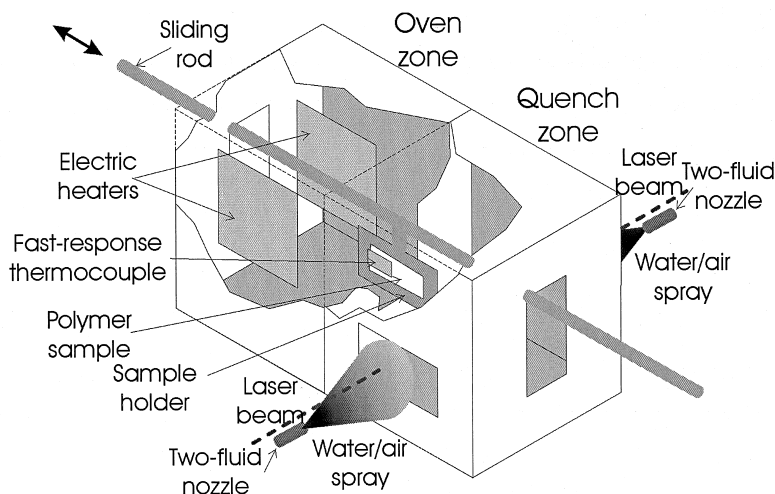
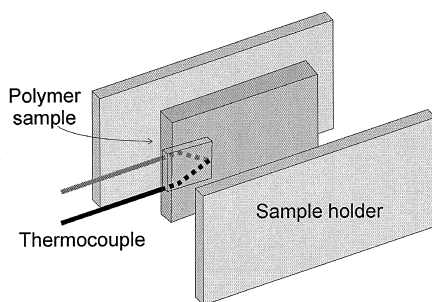


Figure 1. Quenching device scheme

Apparatus description

An apparatus able to quench thin polymer samples (typically, 50-100 microns thickness), and to record crystallization during cooling was developed. A scheme of the apparatus is shown in Figure 1. The apparatus includes a hot (oven zone) section and a cold (quench zone) section, and is equipped with a flat sample holder device that can be quickly shifted from the hot to the cold section. Temperature is measured by a fast response K-type thermocouple (Omega CO1-K, 10 ms response time), inserted directly into the polymer sample. Sample heating is attained by two radiant electric heaters while the cooling system consists of a couple of gas or gas-liquid (typically air and water) operated nozzles (Spraying System, SUJ4B) that spray symmetrically on both faces of sample holder.



As shown in Figures 2, the polymer sample, a thin film with an embedded thermocouple, is confined between two thin glass slides, that work as sample holder. The resulting assembly is fastened to a sliding rod which moves the sample from the oven to the quench zone.

Figure 2. Sample assembly scheme

The apparatus cooling section was designed and realized to determine a large range of cooling rates. Nozzles can be operated with and without water and can be fed at different air pressures and with different water flow rates.

Optical set-up

The real time crystallinity measurement set up is schematically shown in Figure 3. A laser beam, generated by an He-Ne source ($\lambda = 632.8$ nm, 10 mW max output) after the polarizer crosses the sandwiched polymer film while it is subjected to cooling (in the quench zone of the apparatus). Crystallization modifies sample optical properties through two mechanisms which act simultaneously: rotation of light polarization plane and light scattering. Although evaluation of intensity of the depolarized beam downstream from the analyzer could be used to monitor crystallinity evolution, light scattering effects mentioned above were found to interfere with the measurement^[2].

The correction for the scattering effect requires simultaneous detection, downstream from the film under analysis, of both the depolarized beam intensity and the overall beam intensity. In order to perform both these measurements, beyond the sample and upstream to the analyzer the light is splitted in two beams. One beam reaches the first light sensor (photo-resistance, detector 1 in Figure 3) after passing through a crossed polarizer (analyzer), while the other reaches directly the second light sensor (photo-resistance, detector 0 in Figure 3). The main advantage of this technique first reported by Ding and Spruiell^[2] is a very fast response coupled with the non-contact character of the measurements.

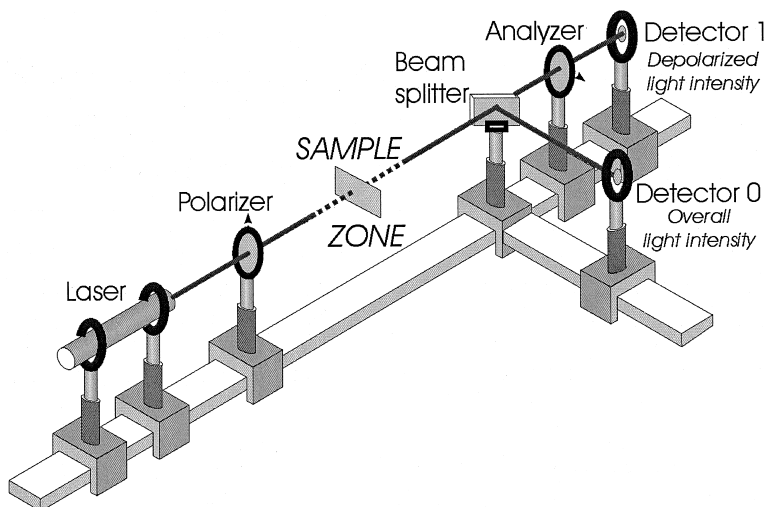


Figure 3. Optical assembly detection scheme adopted for real time crystallization monitoring

Experimental procedure

During the experiment, the polymer is molten and, in order to eliminate memory effects, it is held in the oven section of the apparatus at 240°C for 30 min. Afterward, the sample holder is quickly shifted to the quench section, where it is spray cooled while temperature and light intensities of the two beams are sampled and recorded.

The outputs of the two photo-resistances and thermocouple voltage are continuously recorded by a data acquisition system (National Instruments, PCI 1200) running a specific software code (written in National Instruments LabView 5.0.1, G programming language) developed to synchronize temperature and light intensities data gathering. Sample cooling rates of several hundreds of °C/s have been attained by this apparatus.

Photo-detector tuning

Intensity of incident light changes electrical resistance Ω of a photo-resistor. In particular the higher is the intensity of incident light, the lower is the resistance of the photo-resistor. A linear relationship between light intensity I and electrical conductance $1/\Omega$ is assumed:

$$I = K \left(\frac{1}{\Omega} - \frac{1}{\Omega_b} \right) \quad (1)$$

where K is a calibration constant and Ω_b is the value of the resistance when light source (laser) is off. Because K is not directly accessible to measurement, a calibration procedure was carried out by means of an optical density variable filter. Photo-detector calibration procedure was carried out replacing (in the optical path) the sample with a variable optical density filter. As optical density, OD , of a filter is related to light intensities by:

$$OD = -\log_{10} \left(\frac{I}{I^*} \right) \quad (2)$$

where I and I^* are the filtered and unfiltered beam intensities respectively, the following relationship between photo-resistor electrical conductance and light intensity can be drawn from equations (1) and (2):

$$10^{-OD} = \frac{I}{I^*} = \frac{1/\Omega - 1/\Omega_b}{1/\Omega^* - 1/\Omega_b} \quad (3)$$

where Ω is actual value of photo-resistor electrical resistance and Ω^* is the value measured when $OD = 0$.

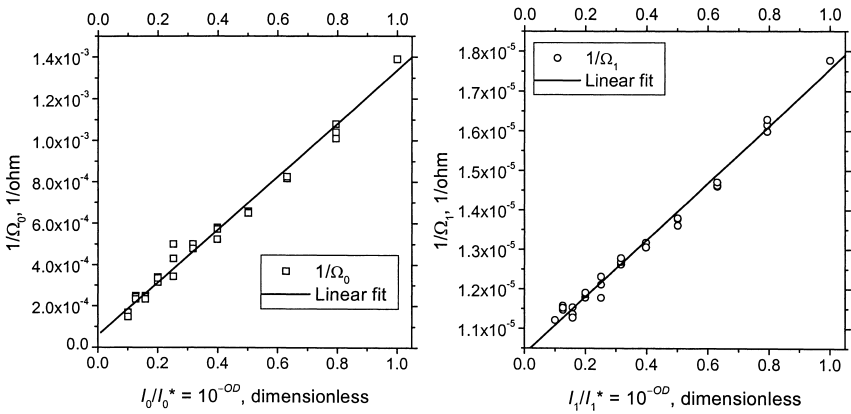


Figure 4. Photo-resistor conductance vs. light intensity ratios for the two photo-resistances: detectors 0 and 1 on the left and the right side respectively

An 11-step filter with 0.1 increments of optical density (L32-599, Edmund Scientific 2001 Catalog, p. 85) was used to calibrate the measurement of incident light intensity. Figure 4 reports calibration curves for both photo-resistors, the data show a linear behavior of conductance versus light intensity of each photo-resistor (linear regression lines are also reported in the figures) confirming that equation (1) can be successfully applied. The values of Ω^* and Ω_b found for both detectors are reported in Table 1.

Table 1. Photo-resistance reference values

	Ω^*	Ω_b
Detector	Ohm	Ohm
0	718	32317
1	56267	96101

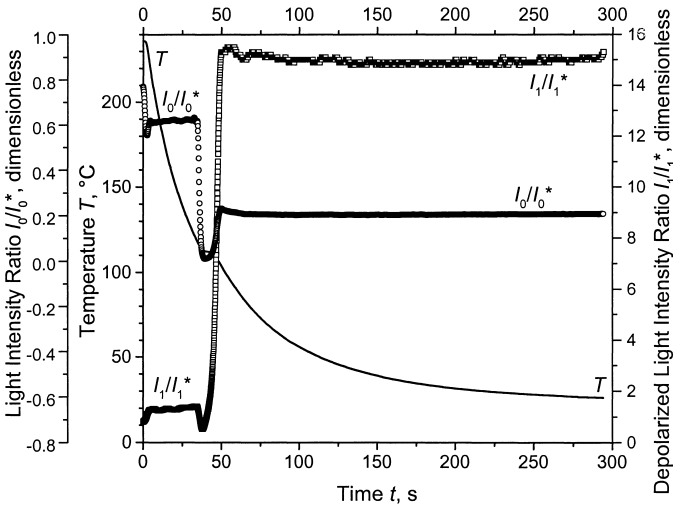


Figure 5. Typical signals output of experiments

Signal analysis

Typical outputs of the quenching experiments for both light intensity ratios as well as temperature are reported in figure 5 as function of time. Light intensity ratios I_0/I_0^* and I_1/I_1^* behave similarly: in the beginning, i.e. before crystallization, they are almost constant, afterward, when crystallization starts up, both signals decrease, pass through a minimum, and then increase, attaining a new level when the crystallization process

terminates. The new level is generally significantly different from the level observed at the beginning of the experiment, i.e. when the beam crosses molten polymer. This behavior, already reported^[2], can be understood taking into account the effect of light scattering by growing crystalline units^[6-8].

At the beginning of the crystallization process the overall emerging light intensity (detector 0), indeed, decreases by effect of the growing number and dimensions of scattering units (polymer spherulites). Afterwards when spherulites start to impinge to each other, reducing the extension of the scattering interface, the overall light intensity increases. The depolarized light intensity (detector 1) on the other hand would be expected to grow continuously during crystallization if overall light intensity were constant; it, vice versa, present a minimum which drives also the depolarized light through a minimum of intensity.

Ding & Spruiell analysis

As suggested in reference^[2], the relative crystallinity $\chi(t)$ can be obtained from relative light intensities according to the following equation:

$$\chi(t) = \frac{X_c(t)}{X_\infty} = \frac{R(t) - R_0}{R_\infty - R_0} \quad (4)$$

where $X_c(t)$ and X_∞ are the crystal volumetric fraction values at time t and at the end of the crystallization process respectively. The relative light intensity is defined as:

$$R(t) = \frac{I_1(t) - I_{lc}}{I_0(t)} \quad (5)$$

Where $I_1(t)$ and $I_0(t)$ are depolarized (detector 1) and the overall (detector 0) light intensities respectively; while I_{lc} is an empirical calibration constant, which accounts of dark signal and polarizing filter effectiveness. $R(t)$, R_0 , and R_∞ in eq. (4) are relative light intensities at time t , at time 0 (the level of the initial plateau) and at the end of the experiment ($t \rightarrow \infty$, the level of the final plateau) respectively.

In the experimental procedure described above absolute values of light intensity are not accessible; rather, intensity ratios are obtained by equation (3) from conductance measurements. Relative light intensities can however be drawn from intensity ratios according to:

$$R(t) = \left(\frac{I_1^*}{I_0^*} \right) \frac{I_1(t) / I_1^* - I_{lc} / I_1^*}{I_0(t) / I_0^*} \quad (5')$$

the value of the ratio I_{lc}/I_1^* (0.0859) was evaluated changing the beam light intensity by

means of a stepped optical density filter located upstream to a birefringent sample (a semi crystalline polymer film). The values of ratios I_1/I_1^* were measured by this procedure versus I_0/I_0^* with different source intensities by interposing four solid polymer films (90 μm thickness) characterized by different crystallinity values. Results are reported in Fig. 6 together with linear regression lines. A very good linear relationship between $I_1(t)/I_1^*$ and $I_0(t)/I_0^*$ was found for the four samples having constant crystallinity and thickness. Moreover, as pointed out by Ding and Spruiell^[2], regression lines cross the ordinate axis in the same point which identifies the ratio I_{1c}/I_1^* .

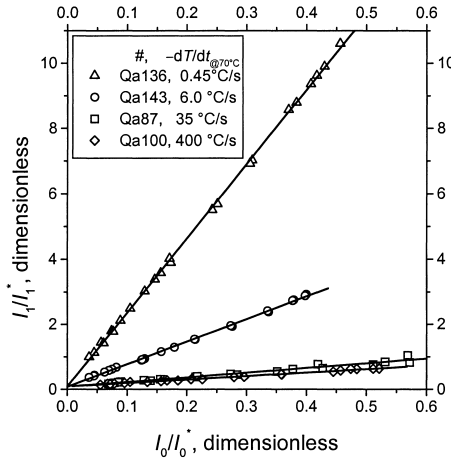


Figure 6. Relative light intensity calibration

The value of the ratio I_{1c}/I_1^* allows the evaluation of a modified relative light intensity $R_R(t)$ as:

$$R_R(t) = \left(\frac{I_0^*}{I_1^*} \right) R(t) = \frac{I_1(t)/I_1^* - I_{1c}/I_1^*}{I_0(t)/I_0^*}, \quad (6)$$

and, finally, of the relative crystallinity $\chi(t)$:

$$\chi(t) = \frac{X_c(t)}{X_\infty} = \frac{R(t) - R_0}{R_\infty - R_0} = \frac{R_R(t) - R_{R0}}{R_{R\infty} - R_{R0}} \quad (7)$$

Thermal analysis

Sample assembly transient thermal problem was analyzed by applying the transient conduction energy balance to an infinite slab accounting for the multiple layer structure of the assembly. The analysis shows that also in the fastest cooling conditions (air/water

sprays) temperature distribution is flat along sample thickness. As a consequence energy balance can be lumped on the slab cross section leading to:

$$\begin{cases} \frac{dT}{dt} = -\frac{1}{\tau}(T - T_{\infty}) \\ @t = t_0 \quad T = T_0 \end{cases} \quad (8)$$

where T_{∞} is temperature of the cooling medium, T_0 is the sample initial temperature (at time t_0) and τ is process time constant, accounting for heat transfer coefficient, geometry and thermal capacity of the assembly. The heat released by crystallization was neglected in equation (8), that is therefore strictly applicable only before and after crystallization takes place. Solution of equation (8), assuming τ constant, leads to:

$$T = T_{\infty} + (T_0 - T_{\infty}) \exp\left(-\frac{t - t_0}{\tau}\right) \quad (9)$$

Although a real cooling history could be well described by a function of several parameters, a single parameter description is commonly preferred for data analysis. The single parameter τ can be evaluated directly from experimental thermal history. Ding and Spruiell^[2] suggested the use of a number of these measures: the cooling rate function (CRF, reciprocal of time constant estimated by fitting thermal history just prior to the crystallization), the average cooling rate and the external heat transfer coefficient. Piccarolo *et al.*^[9] suggested the adoption of a *characteristic* cooling rate, i.e. the cooling rate evaluated at a temperature relevant for crystallization kinetics (temperature at which the crystallization rate constant attains the maximum, 70°C for iPP). Following Piccarolo *et al.*^[9], the iPP cooling histories were characterized by this parameter, easily evaluated from temperature evolution data.

Results and discussion

Several experiments were performed applying different cooling conditions to iPP samples with the aim of testing the apparatus and the method. Some results are reported in Figures 7, 8 and 9 where temperature, light intensity, depolarized light intensity and relative light intensity $R_R(t)$ are reported as function of time for three experiments whose characteristic cooling rates were 0.4, 7.4 and 35 °C/s, respectively.

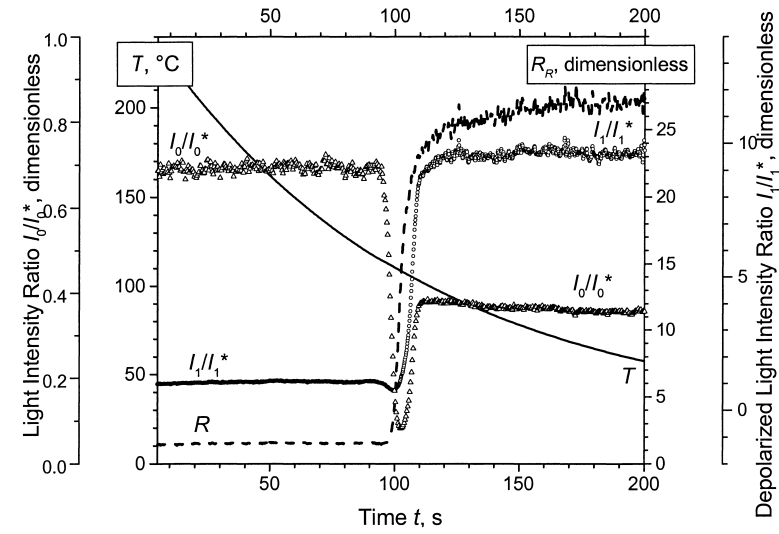


Figure 7. Signals outputs and relative light intensity versus time in experiment Qa154 ($dT/dt_{@70^\circ\text{C}} = -0.40^\circ\text{C/s}$)

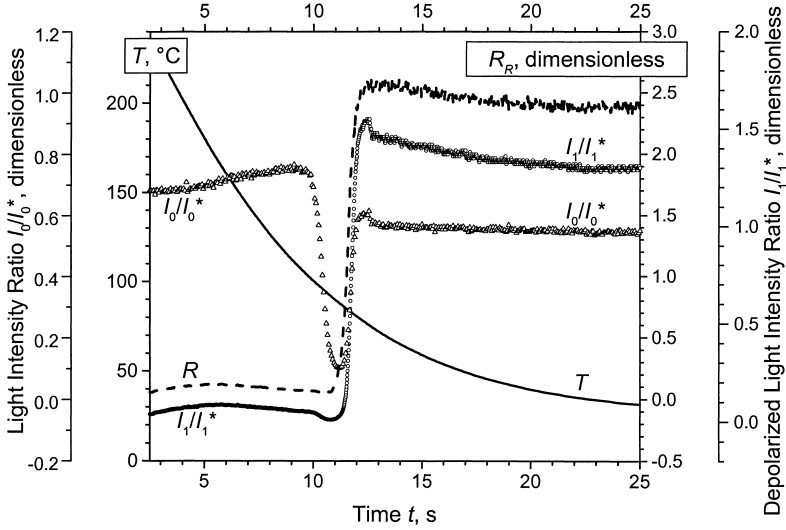


Figure 8. Signals outputs and relative light intensity versus time in experiment Qa151 ($dT/dt_{@70^\circ\text{C}} = -7.4^\circ\text{C/s}$)

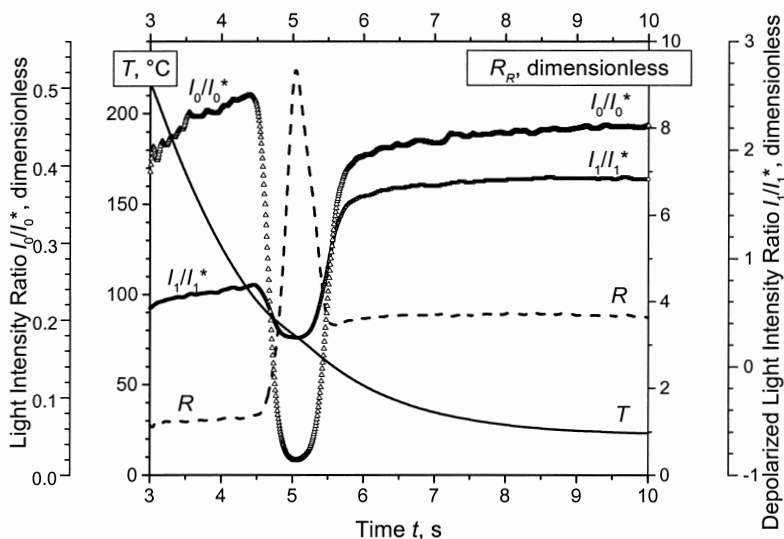


Figure 9. Signals outputs and relative light intensity versus time in experiment Qa164 ($dT/dt_{@70^{\circ}\text{C}} = -35^{\circ}\text{C/s}$)

First of all it is important to outline that: i) the experiment reported in Fig. 7 was carried out at a cooling rate value comparable with the maximum value attained by common calorimetric devices (DSC), ii) data reported in Fig. 8 refers to a cooling history comparable with the fastest that Ding and Spruiell reports as performed by their apparatus, iii) Fig. 9 reports data obtained under a cooling rate about five times larger. In the three experiments here reported, light intensities show the same qualitative behavior outlined in *Signal analysis* section and first reported by Ding and Spruiell results.

Relative light intensity $R_R(t)$ calculated from light intensity ratios $I_1(t)/I_1^*$ and $I_0(t)/I_0^*$ as specified by equation (6) and reported in Figures 7 and 8, shows the expected trend for a property monotonously increasing with crystallinity, i.e. a flat plateau in the beginning of the experiment (molten material) followed by a monotonous increase at intermediate times (crystallization) and finally a second higher plateau at long times (constant crystallinity). Normalization procedure provided by equation (7) leads to results reported in Figure 10 for the relative crystallinity evolution $\chi(t)$. The relative crystallinity evolution $\chi(t)$ curves of these two experiments, indeed, show the expected typical sigmoidal shape. Something puzzling however was observed at higher cooling rates, like in the case of the experiment reported in Figure 9. Although light intensities of

Figure 9 show the same qualitative behavior shown in Figures 7 and 8, relative light intensity and, consequently, relative crystallinity in Figure 10 exhibit a sharp peak rather than a monotonous sigmoidal increase from a low temperature plateau to a high temperature plateau. The same behavior was observed during other experimental runs, carried out also at cooling rates higher than 35°C/s. Such a behavior during a monotonous cooling for a variable which is supposed to represent crystallinity is not physically acceptable. Thus one can conclude that either something is not properly working in the experimental setup signals output or the signals analysis are not properly analyzed.

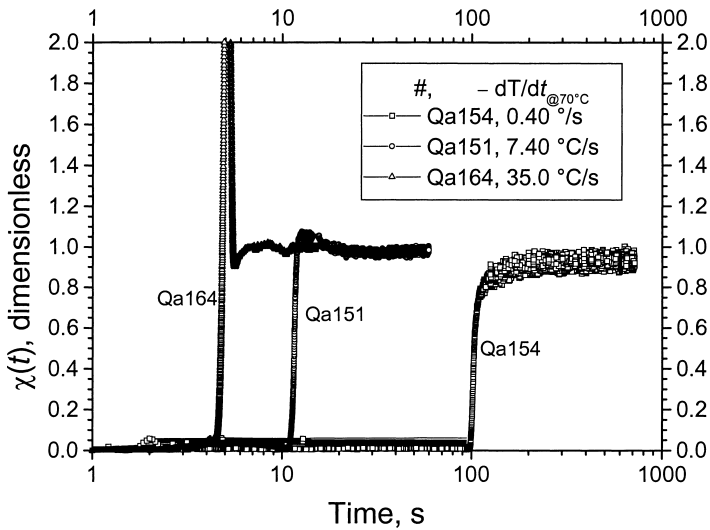


Figure 10. Calculated crystallinity evolution during the following cooling experiments Qa154 ($dT/dt_{@70^{\circ}\text{C}} = -0.40^{\circ}\text{C/s}$), Qa151 ($dT/dt_{@70^{\circ}\text{C}} = -7.40^{\circ}\text{C/s}$) and Qa164 ($dT/dt_{@70^{\circ}\text{C}} = -35.0^{\circ}\text{C/s}$)

Experimental output, however, are simultaneous analysis of the intensities of two fractions of same beam: a simply reflected fraction and what crosses the analyzer downstream to the reflection. Also at the fastest cooling rates adopted, response time of the instruments is several order of magnitude faster than the crystallization phenomenon, thus the two signals $I_1(t)/I_1^*$ and $I_0(t)/I_0^*$ have to be considered as sampled at times essentially equal to each other. On the contrary, optical signal analysis was based on the very simplified lumped model of light scattering and depolarization suggested by Ding and Spruiell^[2] and that model could become inadequate, when

stronger cooling conditions are applied. A more detailed modeling of the light interaction with the sample, taking into account light distribution inside the sample could probably be more appropriate, but it is beyond the scope of this work.

Experiments outputs clearly show the very fast changes that, when crystallization takes place, occur to both overall and depolarized light intensity ratios. These changes identify temperatures at which crystallization starts and ends. Moreover, with reference to the overall light intensity signal, an intermediate peak is always well defined and its temperature can be determined. Usually in DSC measurements the same information is available and the intermediate peak temperature, referred as T_c , is often considered an important parameter outlining crystallization kinetics effects. Also Ding and Spruiell used a parameter related to crystallization phenomenon, i.e. the plateau temperature, read on the thermocouple signal to state the temperature at which crystallization took place.

The peak exhibited by overall light intensity ratio should correspond to the maximum of the scattering phenomenon. Some Authors^[6] ascribe this maximum to a volumetric filling degree (i.e. crystallinity) equal to 50%; therefore, we suggest to adopt the temperature of the overall light intensity ratio peak as a measure of crystallization temperature.

In order to perform a comparison between crystallization temperatures obtained by several authors with different techniques, a single scale for cooling histories needs to be identified. The scale has to account of the section of each cooling history regarding range of temperatures close to that where crystallization occurs. Obviously the $(dT/dt)_{@70^{\circ}\text{C}}$ provide a direct possibility of comparison with DSC experiments, as these are carried out with a constant cooling rate. In the cooling histories adopted in this work, indeed, minor changes of cooling rate occur when crystallization takes place in a range of few tens of $^{\circ}\text{C}$ around 70°C . With reference to Ding and Spruiell work, the authors provide the CRF of their experiments that must be converted into the corresponding $(dT/dt)_{@70^{\circ}\text{C}}$ before comparison. The conversion was here accomplished by fitting their experimental temperature histories by equation (9) and then computing $(dT/dt)_{@70^{\circ}\text{C}}$. The results are reported in Figure 11 and show that a simple linear regression is sufficient to perform the conversion.

Figure 12 reports the crystallization temperature T_c of DSC experiments performed on the same material^[10], the crystallization plateau temperature reported by Ding and

Spruiell^[2] and the overall light intensity (detector 0) peak temperature identified for the experiments performed in the present work as function of $(dT/dt)_{@70^{\circ}\text{C}}$. Superposition of data coming from very different experiments shows a good agreement between the different techniques, confirming that our experimental results can be effectively compared with other sources of crystallization data. It must be outlined, however, that present data extend more than one order of magnitude the maximum cooling rate of experiments with real time monitoring of crystallinity.

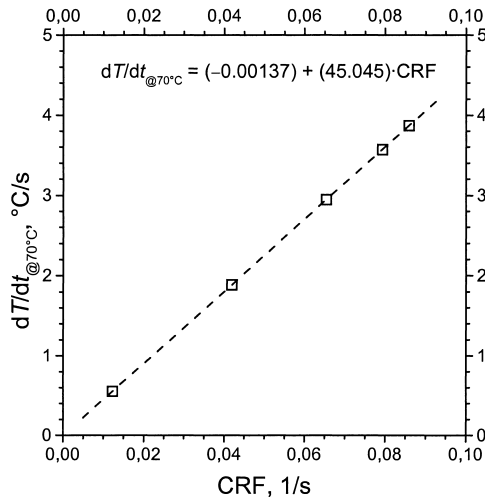


Figure 11. Correlation between cooling rate function CRF and characteristic cooling rate

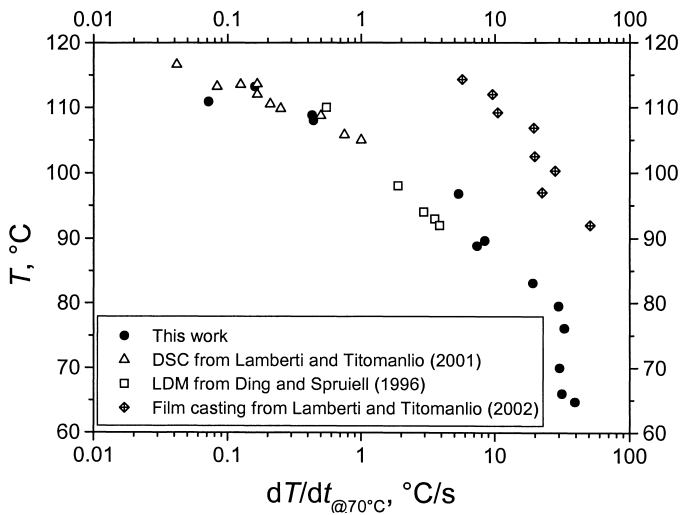


Figure 12. Crystallization temperatures detected with different techniques versus $(dT/dt)_{@70^{\circ}\text{C}}$

During cast film experiments carried out with the same material adopted in this work, a plateau was observed in the temperature distribution along the drawing direction^[11]. The temperature of this plateau, related to heat of crystallization release, is also reported in Figure 12 versus cooling rate at 70°C. The graph clearly shows that crystallization while the film is drawn takes place at temperature about 20°C higher than quiescent crystallization temperature at the same cooling rate. This increase of crystallization temperature is obviously due to the effect of the flow.

Conclusions

An apparatus able to quench thin polymer samples and monitor crystallization evolution during cooling has been built and tested. The apparatus has been employed to drive experiments covering a quite wide range of cooling rates (0.08-35 °C/s).

At low and intermediate cooling rates, signal analysis suggested by Ding and Spruiell was successfully applied obtaining the evolution of crystallinity during the quench. At higher cooling rates the same analysis of both overall and depolarized light intensities downstream from the sample does not give acceptable results for crystallization evolution.

Crystallization temperature was however identified by the experiments at medium-high cooling rates, never explored before.

The apparatus appears to be very promising for the advancement of quiescent crystallization kinetics studies especially if a more detailed analysis of optical signals will allow a reliable description of crystallinity evolution also during quenches carried out with cooling rates of the order of hundred °C/s.

List of Symbols

CRF	Reciprocal of time constant before crystallization
I	Light intensity
I^*	Unfiltered light intensity
$I_0(t)$	Light intensity from detector 0
$I_1(t)$	Light intensity from detector 1
OD	Optical density
$R(t)$	Relative light intensity at time t
R_0	Relative light intensity before crystallization

R_{∞}	Relative light intensity at the final plateau
$R_R(t)$	Modified relative light intensity at time t
t	Time
T_{∞}	Temperature of the cooling medium
T_0	Sample initial temperature
T_c	Intermediate peak temperature
X_{∞}	Crystal volumetric fraction values of the final plateau
$X_c(t)$	Crystal volumetric fraction values at time t
$\chi(t)$	Relative crystallinity at time t
τ	Cooling time constant
$1/\Omega$	Electrical conductance
$1/\Omega_b$	Electrical conductance when light source (laser) is off
$1/\Omega^*$	Electrical conductance with $OD = 0$

- [1] Magill, J.H.; *Polymer*, **1961**, 2, 221, *ibidem*, **1962**, 3, 35
- [2] Ding, Z.; Spruiell, J.E.; *J. Polym. Sci. Part B*, **1996**, 34, 2783, *ibidem*, **1997**, 35, 1077
- [3] Piccarolo, S.; *J. Macromol. Sci. - Phys.*, **1992**, 31, 501
- [4] Brucato, V.; Crippa, G.; Piccarolo, S.; Titomanlio, G.; *Polym. Eng. Sci.*, **1991**, 31, 1411
- [5] Brucato, V.; Piccarolo, S.; Titomanlio, G.; *Makromol. Chem., Macromol. Symp.* **1993**, 68, 245
- [6] Thomas, C.L.; Bur, A.J.; *Polym. Eng. Sci.*, **1999**, 39, 1291
- [7] Samuels, R.J.; *Structured Polymer Properties*, John Wiley & Sons, New York 1974
- [8] Yoon, D.Y.; Stein, R.S.; *J. Polym. Sci. Polym. Phys.*, **1974**, 12, 735
- [9] Piccarolo, S.; Alessi, S.; Brucato, V.; Titomanlio, G.; in *Crystallization of Polymers*, Ed. M. Dosièrè, NATO ASI Series, Kluwer Academic Publisher 1993
- [10] Lamberti, G.; Titomanlio, G.; *Polym. Bulletin*, **2001**, 46, 231
- [11] Lamberti, G.; Titomanlio, G.; paper in this issue of *Macromol. Symp.*, **2002**